LIS1 interacts with CLIP170 to promote tumor growth and metastasis via the Cdc42 signaling pathway in salivary gland adenoid cystic carcinoma

LIJUN LI[1*], ZHIHAO WEN[1*], NI KOU[1,2*], JING LIU[1], DONG JIN[1], LINA WANG[1,2], FU WANG[1-3] and LU GAO[1-3]

[1]School of Stomatology, Dalian Medical University, Dalian, Liaoning 116044; [2]The Affiliated Stomatological Hospital of Dalian Medical University School of Stomatology, Dalian, Liaoning 116027; [3]Academician Laboratory of Immune and Oral Development and Regeneration, Dalian Medical University, Dalian, Liaoning 116044, P.R. China

Received April 16, 2022; Accepted August 5, 2022

DOI: 10.3892/ijo.2022.5419

Abstract. Salivary gland adenoid cystic carcinoma (SACC) is one of the most common malignant tumors, with high aggressive potential in the oral and maxillofacial regions. Lissencephaly 1 (LIS1) is a microtubule-organizing center-associated protein that regulates the polymerization and stability of microtubules by mediating the motor function of dynein. Recent studies have suggested that LIS1 plays a potential role in the malignant development of tumors, such as in mitosis and migration. However, the role of LIS1 in SACC development and its related molecular mechanisms remain unclear. Thus, the effects of LIS1 on the proliferation, apoptosis, invasion and metastasis of SACC were studied, *in vivo* and *in vitro*. The results of immunohistochemical staining showed that LIS1 was highly expressed in SACC tissues, and its expression level was associated with malignant progression. *In vitro*, the results of CCK-8, TUNEL, wound healing and Transwell assays demonstrated that LIS1 promotes proliferation, inhibits apoptosis, and enhances the migration and invasion of SACC-LM cells. *In vivo*, knockdown of LIS1 effectively suppressed the growth of subcutaneous tumors in a mouse xenograft and distant metastasis of tumor cells in the metastasis model. The co-immunoprecipitation, immunofluorescence and western blot results also revealed that LIS1 binds to cytoplasmic linker protein 170 (CLIP170) to form a protein complex (LIS1/CLIP170), which activates the cell division control protein 42 homolog (Cdc42) signaling pathway to modulate the proliferation and anti-apoptosis of tumor cells, and enhanced invasion and metastasis by regulating the formation of invadopodia and the expression of MMPs in SACC-LM cells. Therefore, the present study demonstrated that LIS1 is a cancer promoter in SACC, and the molecular mechanism of the LIS1/CLIP170/Cdc42 signaling pathway is involved in the malignant progression, which offers a promising strategy for targeted therapy of SACC.

Correspondence to: Dr Fu Wang or Dr Lu Gao, School of Stomatology, Dalian Medical University, 9 West Section Lvshun South Road, Dalian, Liaoning 116044, P.R. China
E-mail: fuwang@dmu.edu.cn
E-mail: dygaolu@dmu.edu.cn

*Contributed equally

Key words: salivary gland adenoid cystic carcinoma, lissencephaly 1, cell division control protein 42 homolog, microtubule-associated protein, malignancy, metastasis

Introduction

Salivary adenoid cystic carcinoma (SACC) is a common malignant tumor of the major and minor salivary glands, accounting for 30% of salivary gland epithelial malignant tumors. Due to its biological characteristics, such as nerve and vascular invasion, distant metastasis and high recurrence rate, the 15-year survival rate of patients is only 40% (1-3). At present, the effective treatment for SACC mainly includes surgery and radiotherapy. Little is known about the targeted therapy for identifying potential molecular abnormalities in SACC. Further investigation of the specific mechanism underlying malignant progression of SACC is urgently needed to provide new and effective therapeutic targets.

Malignant proliferation, invasion and metastasis of tumor cells is a complex process that requires extensive reorganization of the cytoskeleton. A high frequency of intracellular cytoskeleton reorganization has been observed in cancer, including actin cytoskeleton remodeling, microtubule rearrangement and intermediate filament changes (4-6). Throughout the remodeling process, these transformations are usually controlled by microtubule-related proteins (7,8). Therefore, microtubule regulatory proteins play a potential role in the malignant progression of tumors, such as in cell division, cell polarization, and cell migration. Lissencephaly 1 (LIS1), also known as platelet-activating factor acetylhydrolase 1b1 (PAFAH1B1), is a microtubule-organizing center-associated protein that regulates the polymerization and stability of microtubules by mediating the motor function of dynein (9).

Through in situ hybridization, Allanson *et al* (10) found that the LIS1 gene was heterozygous in patients with Miller Dieker syndrome (MDS). The syndrome is a typical anencephalic malformation, which is a brain malformation caused by abnormal neuronal migration. LIS1 is a regulated adapter between cytoskeleton-associated proteins and cytoplasmic dynein at sites involved in cargo microtubule loading and in the control of microtubule dynamics, which participates in a series of cell activities, including cell migration, organelle location and spindle assembly (9). Previous studies have found that LIS1 is highly expressed in tumor tissues. The expression of LIS1 in lung cancer tissue was demonstrated to be significantly correlated with the occurrence and prognosis of lung cancer. LIS1 promoted lung cancer cell invasion and metastasis by regulating the aggregation of microtubules and fibronectin (11); in cholangiocarcinoma, miR-144 targeted LIS1 mRNA and suppressed the proliferation and invasion of tumor cells (12). However, the mechanism by which LIS1 regulates tumor cells is unclear.

Previous studies have reported that there is a physical interaction between the WD-40 domains of LIS1 and the zinc fingers of cytoplasmic linker protein 170 (CLIP-170) and provided evidence that LIS1 plays a novel role in mediating CLIP-170/dynein interactions and in coordinating dynein cargo-binding and motor activities (13). CLIP170 is a microtubule-associated protein with a cytoskeleton-associated protein glycine-rich (CAP-Gly) domain. The second zinc finger of its COOH-terminus has been implicated in the interaction with microtubule plus-end-tracking proteins (+TIPs) to participate in various cellular processes, including regulation of microtubule dynamics, cell migration and intracellular transport (14). Several previous studies have implicated CLIP-170 in the pathogenesis of cancer. CLIP-170 was revealed to increase the ability of paclitaxel to block cell cycle progression at mitosis and to induce apoptosis in breast cancer cells (15). A previous study by the authors demonstrated that arsenic trioxide (ATO) disrupted the zinc finger of CLIP170 to disturb the LIS1/NDEL1/dynein microtubule dynamic complex, thus inhibiting the ability of migration and invasion in head and neck cancer (16). However, the specific downstream mechanism of the LIS1/CLIP170 complex regulating the progression of tumor cells remains unknown.

Cell division control protein 42 homolog (Cdc42) is a member of the Rho family of small GTPases and a master regulator of the actin cytoskeleton, controlling cell motility, polarity and cell cycle progression (17). Cdc42 is upregulated in several human cancer cell lines and its expression has been demonstrated to be correlated with tumor stage, lymph node metastasis, and patient survival (18,19). A previous study revealed that Cdc42-mediated phosphorylation of CLIP-170 was essential for the normal function of this protein during cell cycle progression (20). CLIP-170 interacted with IQ motif containing GTPase activating protein 1 (IQGAP1), an effector of Cdc42, leading to a polarized microtubule array and formation of cell tight junctions (TJ) (21). The direct downstream effector of Cdc42 was revealed to regulate cell migration and invasion via actin polymerization, pseudopodia formation, and matrix metalloproteinase (MMP) secretion (22). Inhibition of Cdc42 in Ras-transformed cells was shown to decrease oncogenic signaling via Akt, thus contributing to the reduction of cancer malignancy (23). Therefore, the role of Cdc42 in cancer has been well established but its mechanism with the LIS1/CLIP170 complex has yet to be fully elucidated.

In the present study, the expression and distribution of LIS1 in SACC was first detected. Next, the effects of LIS1 on the proliferation, apoptosis, invasion and metastasis of SACC were studied, *in vivo* and *in vitro*. On this basis, the molecular mechanism by which LIS1 interaction with the +TIP, CLIP-170, regulates the malignant progression of SACC through the Cdc42 signaling pathway was further explored. The results provide mechanistic insights into microtubule-associated cellular processes and their pathological function in SACC, and also provide a theoretical foundation for a new therapeutic target.

Materials and methods

Human SACC tissues. A total of 30 human SACC tissues and 20 normal and adjacent tissues were collected at the Second Affiliated Hospital of Dalian Medical University from June 2017 to September 2019. The patients diagnosed with SACC were included with no restrictions in terms of age and sex, but excluded with treatment of radiotherapy or chemotherapy. The related clinical information is listed in Table SI. The procedures of the present study concerning human subjects were approved (approval no. DY2021-005) by the Medical Ethics Committee of Dalian Medical University (Dalian, China), and written informed consent was provided by each patient.

Immunohistochemistry (IHC) and evaluation. Immunohistochemical staining was performed according to procedures described in a previous study by the authors (24). Briefly, 4-μm thick sections were deparaffinized in dimethylbenzene and rehydrated in graded ethanol after baking at 65˚C for 1 h. Following antigen retrieval, 3% hydrogen peroxide solution was used to inactivate endogenous peroxidase for 15 min at room temperature. After being blocked with goat serum for 30 min at 37˚C, tissues were incubated overnight at 4˚C with a primary antibody: LIS1 (1:200; product code ab2607; Abcam); Ki67 (1:3,000; cat. no. 27309-1-AP; ProteinTech Group, Inc.); Pan-CK (1:3,000; cat. no. 26411-1-AP; ProteinTech Group, Inc.) MMP2 (1:200; product code ab86607; Abcam); MMP9 (1:200; product code ab38898; Abcam); and MMP14 (1:100; product code ab78738; Abcam). The following day, the secondary antibody and horseradish peroxidase streptavidin (both contained in a kit; 1:1; cat. no. SAP-9100; ZSGB-BIO, Inc.) were added to the slices for 30 min at 37˚C. The sections were then incubated with 3,3'-diaminobenzidine (DAB; ZSGB-BIO, Inc.) as a chromogen substrate and counterstained with hematoxylin for 3 min at room temperature. Finally, the slices were dehydrated with graded ethanol, cleared with xylene and mounted with neutral gum (Solarbio Science & Technology, Co., Ltd.). For the evaluation, images were obtained using a phase microscope (Olympus Corporation), and the integral optical density (IOD) and the positive immunohistochemical staining region were measured with Image-Pro Plus 7.0 software (Media Cybernetics, Inc.). Protein expression was semi-quantitatively calculated and classified based on the intensity of staining and the percentage of stained cells as previously described (25).

Cell culture and transfection. The SACC-LM cell line was a kind gift from Professor Liu (Affiliated Stomatological Hospital of Fudan University, Shanghai, China) (3) and was cultured in DMEM/F12 supplemented with 10% fetal bovine serum (FBS; ScienCell Research Laboratories, Inc.), 100 U/ml penicillin and 100 U/ml streptomycin (Gibco; Thermo Fisher Scientific, Inc.) at 37˚C in a humidified atmosphere with 5% CO_2. The plasmids, including the pc-DNA3.1 vector and plasmids encoding LIS1 and CLIP170 were constructed by Changsha YouBio Co., Ltd. The small interfering RNAs (siRNAs) were purchased from Shanghai GenePharma Co., Ltd. and the target sequences are provided in Table SII. The cells were seeded into 6-well plates at $4x10^5$ cells per well and cultured to 70-80% confluence. Lipofectamine 3000 Transfection Reagent (3.75 μl; cat. no. L3000015; Invitrogen; Thermo Fisher Scientific, Inc.) was used for cell transfection with 2,500 ng plasmids or 37.5 pmol siRNAs. The transfection system was incubated for 8 h at 37˚C. The subsequent experiment was performed at 24 h after transfection. In addition, siRNA scramble (si-control, Shanghai GenePharma Co., Ltd.) was used as the negative control.

Reverse transcription-quantitative polymerase chain reaction (RT-qPCR). Total RNA was extracted from SACC-LM cells with RNAiso Plus (TRIzol; Takara Bio, Inc.), and then, reverse transcription into cDNA was performed using a PrimeScript RT reagent Kit (Takara Bio, Inc.) according to the manufacturer's instructions. The primer sequences for RT-qPCR are provided in Table SIII. GAPDH was used as the internal control for each experiment. RT-qPCR was performed with SYBR Premix Ex Taq (Tli RNaseH Plus; Takara Bio, Inc.). The PCR conditions were as follows: Initial denaturation at 95˚C for 30 sec, followed by 40 cycles of denaturation at 95˚C for 5 sec, annealing at 55˚C for 30 sec and elongation at 72˚C for 30 sec, and then a final extension at 72˚C for 5 min. The data were collected with a TP800 system (Takara Bio, Inc.) and analyzed using the $2^{-\Delta\Delta Cq}$ comparative method (26).

Cell viability assay. Cell proliferation was assessed using Cell Counting Kit-8 (CCK-8; APeXBio Technology, LLC). According to the manufacturer's instructions, cells were seeded in a 96-well plate at a density of $1x10^3$ cells/well in 100 μl of culture medium for 0-48 h. CCK-8 solution (10 μl) was added to each well of the plate, and then, the plate was incubated for 1 h in an incubator at 37˚C. Finally, the absorbance was measured at 490 nm using a microplate reader (Shanghai Flash Spectrum Biotechnology Co., Ltd.).

5'-Ethynl-2'-deoxyuridine (EdU) staining assay. An EdU assay kit (product code ab219801; Abcam) was used to assess cell proliferation. Following cell dissociation, the cells were diluted to $1x10^6$ cells/ml with culture medium and labeled with EdU solution for 4 h. The cells were then fixed with 4% paraformaldehyde for 15 min at room temperature, permeabilized in permeabilization buffer and incubated with EdU reaction mix at room temperature for 30 min. Finally, the number and proportion of EdU-incorporated cells were analyzed on a flow cytometer (FACSVerse; BD Biosciences) at Ex/Em=491/520 nm. The data were analyzed using Cell Quest software v5.1 (BD Biosciences).

Terminal deoxynucleotidyl transferase dUTP nick-end labeling (TUNEL) staining. For cell samples, following transfection, the cells were seeded onto coverslips. After adherence, the cells were fixed with 4% paraformaldehyde for 20 min at 37˚C and then permeabilized with 0.25% Triton X-100 in PBS for 5 min. For 5 μm paraffin sections, after deparaffinization and rehydration, the tissues were permeabilized with 20 μg/ml Proteinase K in PBS for 5 min according to the instructions of a TUNEL Bright Apoptosis Detection Kit (cat. no. A112-01; Vazyme Biotech, Co., Ltd.) and a previous study by the authors (27). Briefly, the sections were incubated with the Equilibration Buffer for 30 min at room temperature and then marked with the labeling mix buffer for 1 h at 37˚C. Finally, the sections were mounted with 4',6-diamidine-2'-phenylindole dihydrochloride (DAPI; 1:1,000; cat. no. 10236276001; Roche Diagnostics) at 37˚C for 10 min, and five visual fields were randomly selected for observation using fluorescence microscopy (Olympus Corporation).

Wound healing assay. Following transfection with LIS1 or si-CLIP170, SACC-LM cells were seeded in 6-well plates at a density of $5x10^5$ cells per well with or without treatment of ML141 (Cdc42 inhibitor; MedChemExpress). A 200-μl pipette tip was used to create scratches in the cell monolayer when cells were merged to 75-80% confluence. The cells were then washed with PBS and cultured in serum-free medium. Images were obtained using a light microscope (Olympus Corporation) at 0, 12 and 24 h to record the wound area. Finally, the area of cell migration was quantified using Image-Pro Plus 7.0 software.

Cell migration and invasion assays. For the cell migration and invasion assays, cells ($5x10^3$/well) in 200 μl serum-free medium were directly seeded into the upper chambers (pore size, 8 μm; Corning, Inc.) coated with (at 37˚C for 1 h; for the invasion assay) or without (for the migration assay) Matrigel (Corning, Inc.). Subsequently, 800 μl medium with 20% FBS was added to the lower chambers. Following culture for 12 or 24 h in an incubator, the cells were fixed with 4% paraformaldehyde (Solarbio Science & Technology, Co., Ltd.) for 20 min at 37˚C and then stained with 1% crystal violet (Beijing Coolibo Technology Co., Ltd.) for 10 min at room temperature. The upper surface of the membranes was wiped with a cotton swab to remove the non-penetrating cells. Under a phase microscope at a high magnification (x200), five fields in each sample were randomly selected, and the number of migrated or invasive cells was counted.

Immunofluorescence (IF) staining. Invadopodia of tumor cells were detected by colocalization of cortactin and F-actin according to a previous study by the authors (28). Cells were fixed with 4% paraformaldehyde for 20 min at 37˚C, washed three times with PBS, and then permeabilized with 0.25% Triton X-100 in PBS for 15 min at room temperature. Following washing, the cells were blocked with 2.5% bovine serum albumin (BSA; Solarbio Science & Technology, Co., Ltd.) for 1 h at 37˚C and stained with the primary antibody, cortactin (1:1,000; product code ab81208; Abcam) overnight at 4˚C. Following three washes, the cells were incubated with Alexa Fluor 488 secondary antibody (1:400; cat. no. A-11034;

Thermo Fisher Scientific, Inc.) and rhodamine-conjugated phalloidin (1:400; product no. 40734ES75; Yeasen Biotechnology Co., Ltd.) at 37˚C for 1 h. Finally, the cell nuclei were counterstained with DAPI (Roche) for 5 min at room temperature away from light, and the coverslips were mounted with fluorescence decay resistance medium (Solarbio Science & Technology, Co., Ltd.). The sections were observed and images were captured using a confocal microscope (Leica Microsystems, Inc.). For evaluation, five random high-power fields were selected, and the threshold was set based on the staining of the negative control. Colocalization of cortactin and F-actin was considered to indicate invadopodia formation. The area of invadopodia per cell was quantitatively calculated using Image-Pro Plus 7.0 software.

Western blotting. Cells ($2x10^6$) were lysed using radioimmunoprecipitation assay lysis buffer (RIPA; Solarbio Science & Technology, Co., Ltd.) and assessed with a bicinchoninic acid protein assay kit (BCA; Beyotime Institute of Biotechnology). Subsequently, 20 μg protein was loaded into a 10% polyacrylamide gel, separated by electrophoresis and transferred to a polyvinylidene difluoride membrane (PVDF; Millipore; Merck KGaA). The membrane was blocked with 5% non-fat milk for 1 h at room temperature and incubated with a primary antibody at 4˚C overnight: GAPDH (1:6,000; cat. no. 60004-1-lg; ProteinTech Group, Inc.); LIS1 (1:1,000; product code ab2607; Abcam); CLIP170 (1:1,000; product code ab61830; Abcam) MMP2 (1:1,000; product code ab86607; Abcam); MMP9 (1:1,000; product code ab38898; Abcam); MMP14 (1:500; product code ab78738; Abcam); BCL2 (1:1,500; cat. no. 12789-1-AP; ProteinTech Group, Inc.); cyclin D1 (1:250; cat. no. sc-8396; Santa Cruz Biotechnology, Inc.); Cdc42 (1:1,000; product code ab187643; Abcam) and then the secondary HRP-conjugated antibody (1:2,000; cat. no. ZB-2305; ZSGB-BIO, Inc.) at room temperature for 1 h. Finally, the proteins on the membranes were visualized using a Supersignal West Femto Kit (cat. no. 34094; Thermo Fisher Scientific, Inc.) and scanned with an imager (ChemiDoc™ Touch Imaging System; Bio-Rad Laboratories, Inc.). The ImageJ software (version 1.51j8; National Institutes of Health) was used for densitometric analysis.

Recombinant lentiviruses and stable cell lines. Full-length cDNA encoding human LIS1 was cloned into pLenti-CMV-EGFR-Puro with an HA tag. The LIS1 short hairpin RNA (sh-LIS1) and shRNA scramble as the negative control (sh-control) were constructed using GV248-EGFP-Puro. The sh-LIS1 target sequence was 5'-GCATGTGGTAGAATG CATT-3', and the sh-control target sequence was 5'-TTCTCC GAACGTGTCACGT-3'. The 3rd generation system was used to recombine lentiviruses, and 2.5 μg transfer plasmid, 1.25 μg pMDLg/RRE, 0.75 μg VSVG and 0.5 μg pRSV-Rev were transfected into 293FT cells (cat. no. R70007; Thermo Fisher Scientific, Inc.) in a 6-cm dish for 8 h at 37˚C. The culture medium with recombinant lentiviruses was collected after 24 and 48 h of transfection. Lentiviruses with plasmids and sh-RNA were provided by Shanghai GeneChem Co., Ltd. and used to infect SACC-LM cells at a multiplicity of infection (MOI) of 10 for 48 h at 37˚C. Stable cell lines were selected with 10 μg/ml puromycin (Beijing Coolibo Technology Co., Ltd.) for 4 weeks. The expression of LIS1 in SACC-LM cells was detected by qPCR and western blotting.

In vivo animal experiments. A total of 40 female nude mice (BALB/c; 4 weeks old; weight, 18-20 g) were obtained from Dalian Medical University Laboratory Animal Center. The animal experiments were approved (approval no. AEE20017) by the Animal Experimental Ethics Committee of Dalian Medical University. The 40 mice were housed at 23±2˚C and 50±10% humidity, and under a 12-h light/dark cycle with access to food and water *ad libitum*. The mice were divided into eight groups randomly (4 groups for the xenograft models and 4 groups for the metastasis models). For the xenograft models, $1x10^7$ SACC cells stably transfected with vector, LIS1, sh-control and sh-LIS1, respectively, in 100 μl PBS were subcutaneously injected into the right flank of the mice (n=5 per group) under anaesthetization by an intraperitoneal injection of sodium pentobarbital (30 mg/kg). The volume of the tumor (length x width^2/2) (29) and the weight of the mice were monitored every two days throughout the study period. In compliance with the Guide for the Animal Care and Use Committee (ACUC) from the US National Institutes of Health, all tumor burdens were not >10% body weight of the mice, and the maximum tumor volume was 751.04 mm^3. After 1 month, the 20 mice were euthanized through the intravascular administration of an overdose of sodium pentobarbital (>100 mg/kg) followed by cervical dislocation. Euthanasia was confirmed by the loss of vital signs (respiration and heartbeat cessation), and the harvested tumors were separated and fixed with 4% paraformaldehyde at 4˚C for 48 h for subsequent histochemical staining. For the metastasis models, $5x10^6$ SACC cells stably transfected with vector, LIS1, sh-control and sh-LIS1, respectively, in 100 μl PBS were injected into the mice via the tail vein (n=5 per group) under anaesthetization by an intraperitoneal injection of sodium pentobarbital (30 mg/kg). The mice were weighed and observed every other day. After one month, an IVIS Spectrum system (PerkinElmer, Inc.) was used to detect tumor metastasis by tracking cells with stable green fluorescent protein. Living Image Software (version 4.4; PerkinElmer, Inc.) was used to quantify tumor metastasis. According to the humane endpoints in ACUC, among the 20 metastasis model mice, 10 mice were euthanized through the intravascular administration of an overdose of sodium pentobarbital (>100 mg/kg) followed by cervical dislocation in advance due to adverse complications (loss of body weight >20% and uncoordinated movement) after tail vein injection of tumor cells, and the other 10 mice were euthanized at two months after injection. The lungs of the mice were then isolated and fixed for subsequent immunohistochemical staining.

Co-immunoprecipitation (IP). Following transfection, the cells in 6-well plates were lysed with 300 μl IP lysis buffer (Thermo Fisher Scientific, Inc.) per well at 4˚C for 5 min. The lysis buffer was then centrifuged for 13,000 x g at 4˚C for 10 min to obtain the supernatant. All samples were processed using a Pierce Co-Immunoprecipitation (Co-IP) Kit (cat. no. 88804; Thermo Fisher Scientific, Inc.) according to the manufacturer's recommendations. Cell lysates were incubated

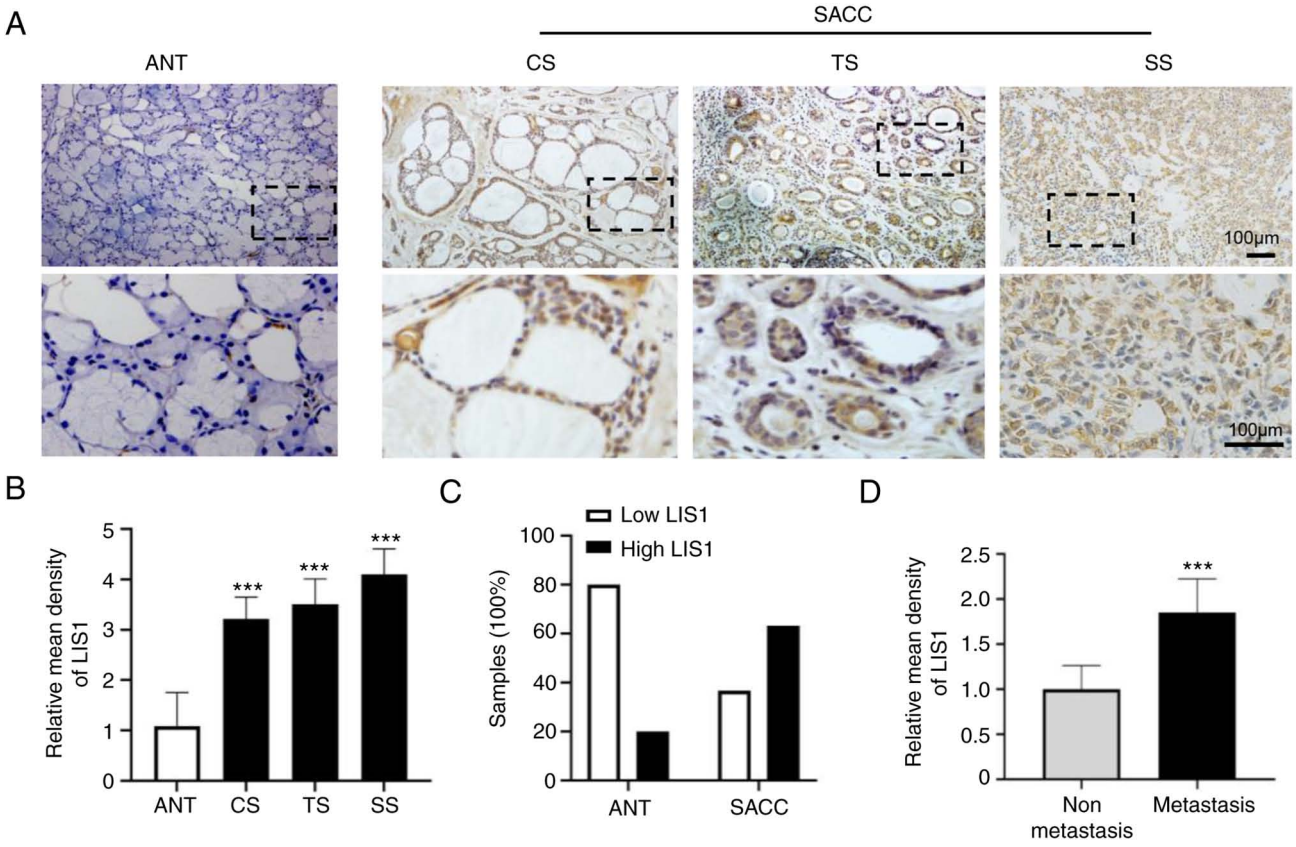

Figure 1. Abundant expression of LIS1 in human SACC tissues. (A) Immunohistochemical staining of LIS1 in ANT, CS, TS, and SS tissue. Shown in the bottom row are enlarged images of the dashed region above. Scale bar, 100 μm. (B) Quantitative analysis of LIS1 expression in ANT and SACC samples. (C) The proportion of ANT and SACC samples with low or high LIS1 expression. (D) Quantitative analysis of LIS1 expression in metastatic and non-metastatic SACC samples. Mean ± SEM; ***P<0.001. LIS1, lissencephaly 1; SACC, salivary gland adenoid cystic carcinoma; ANT, adjacent normal tissue; CS, cribriform SACC; TS, tubular SACC; SS, solid SACC.

with a primary antibody: LIS1 (1:50; product code ab2607, Abcam); or CLIP170 (1:50; product code ab61830; Abcam), overnight at 4˚C, and then, the antigen and antibody complexes were combined with 250 μg protein A/G magnetic beads at room temperature for 1 h. After the beads were collected by a magnetic stand, the complexes were eluted for 10 min, and the expression of immunoprecipitated proteins was detected by western blotting.

Statistical analysis. All statistical analyses were performed using GraphPad Prism 7 (GraphPad Software, Inc.). Unpaired two-tailed t-test was used for two groups, and one-way analysis of variance followed by Tukey's post hoc test was used for multiple comparisons. Kaplan-Meier with log-rank testing was performed for the survival analysis of the mice. All experiments were performed at least in triplicate. All data are presented as the mean ± SEM. P<0.05 was considered to indicate a statistically significant difference.

Results

Abundant expression of LIS1 in SACC. To evaluate whether LIS1 is a therapeutic target for a promising SACC treatment strategy, the expression and distribution of LIS1 in the tissues and adjacent normal tissues (ANTs) of patients with SACC were examined using IHC staining. As shown in Fig. 1A, the expression of LIS1 was markedly increased in most SACC tissues compared with ANTs. The results also revealed that the positive staining area of LIS1 was mainly localized in the cytoplasm of cancer cells rather than in the nucleus. By analyzing the mean density of LIS1, it was determined that there was significantly higher LIS1 expression in SACC tissues than in ANTs. SACC consists of two main cell types: Ductal and modified myoepithelial cells. These two types of cells exhibited three basic growth patterns: Cribriform, tubular, and solid. Among the three patterns, it was determined that the expression level of LIS1 was higher in solid SACC tissues (low differentiation) than in the other two pattern types (high differentiation) (Fig. 1B).

In addition, the proportion of high and low LIS1 expression levels were analyzed in ANTs and SACC (Table SI). The results revealed that in ANTs, the proportion with low and high LIS1 expression was 80 and 20%, respectively. By contrast, low expression of LIS1 accounted for only 36.67%, and high expression of LIS1 was as high as 63.33% in SACC samples (Fig. 1C). Moreover, the expression level of LIS1 was examined in metastatic and non-metastatic samples and it was determined that the expression of LIS1 was significantly higher in metastatic samples than in non-metastatic samples (Fig. 1D). In summary, the aforementioned results indicated that LIS1 was highly expressed in SACC and that its level was positively associated with the malignancy of SACC.

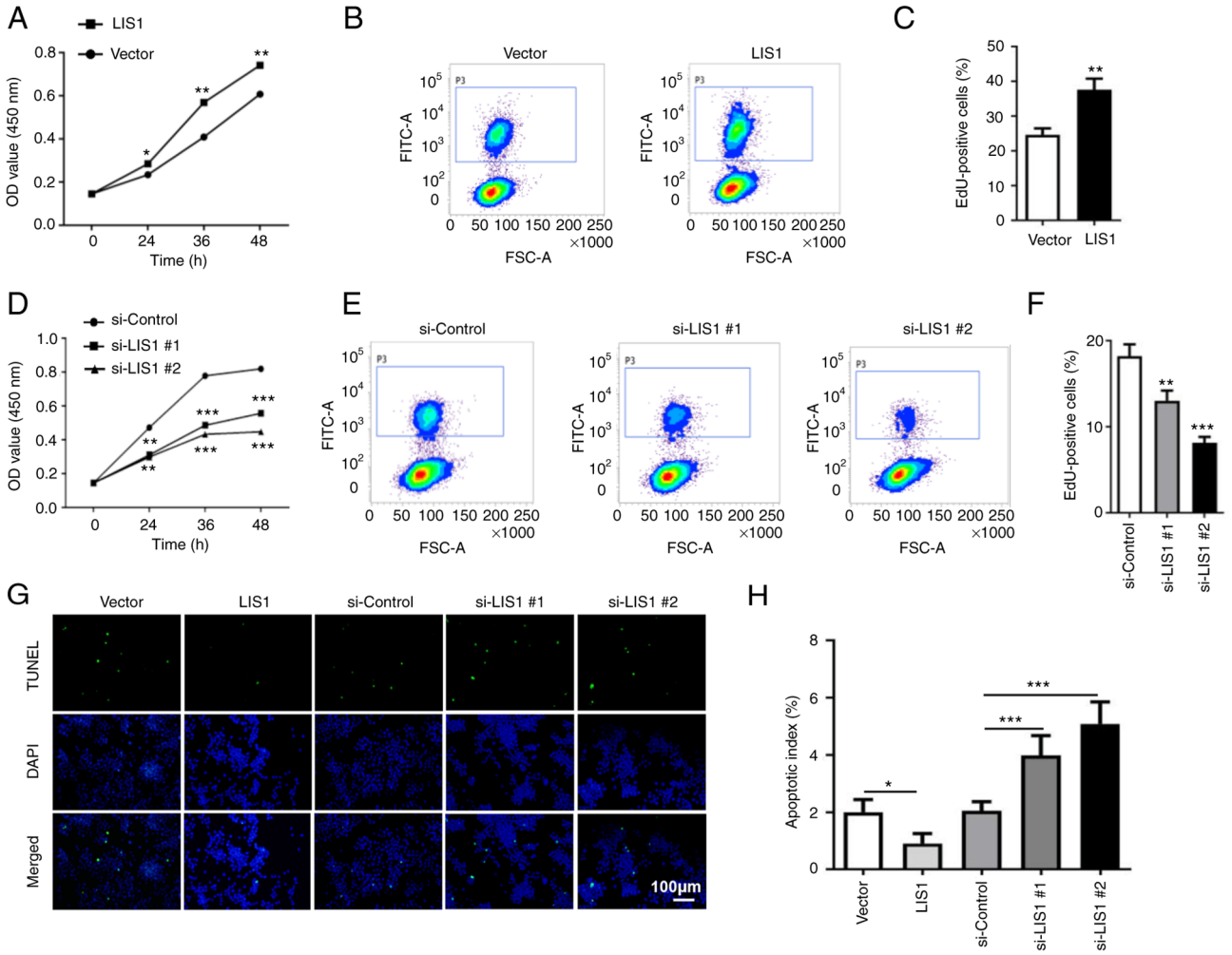

Figure 2. LIS1 promotes the proliferation and anti-apoptosis of SACC-LM cells. (A and D) Cell proliferation was examined via CCK-8 assays in SACC-LM cells transfected with (A) LIS1 overexpression plasmid or (D) si-LIS1. (B and E) The proliferation of SACC-LM cells was detected by EdU assays at 48 h after transfection with the (B) LIS1 overexpression plasmid or (E) si-LIS1. (C and F) Quantitative statistical analysis of the EdU assay results. (G) TUNEL assays were performed to assess cell apoptosis at 48 h after overexpression or siRNA targeting LIS1 in SACC-LM cells. Scale bar, 100 μm. (H) Quantitative statistical analysis of TUNEL assay results. Mean ± SEM; *P<0.05, **P<0.01 and ***P<0.001. LIS1, lissencephaly 1; SACC, salivary gland adenoid cystic carcinoma; CCK-8, Cell Counting Kit-8; si-, small interfering RNA; EdU, 5'-ethynl-2'-deoxyuridine; TUNEL, terminal deoxynucleotidyl transferase dUTP nick-end labeling.

LIS1 promotes proliferation and anti-apoptosis of SACC-LM cells. To investigate the effect of LIS1 on SACC-LM cells, LIS1 overexpression plasmids were first constructed for transient transfection and siRNAs targeting the human LIS1 sequence were employed to overexpress and knock down LIS1 in SACC-LM cells, respectively (Fig. S1A-D). As shown in Fig. 2A and D, CCK-8 assays revealed that overexpression of LIS1 significantly enhanced the proliferation ability of tumor cells compared with the control group, while knockdown of LIS1 (si-LIS1) significantly suppressed cell proliferation. EdU incorporation assays revealed that the percentage of EdU-positive cells was higher at 48 h after transfection with the LIS1 plasmid than after transfection with the vector plasmid (Fig. 2B and C). In the si-LIS1 group, the percentage of EdU-positive cells was significantly decreased compared with that in the si-control group (Fig. 2E and F). The effect of LIS1 was further explored on the apoptosis of SACC-LM cells using TUNEL assays at 48 h after transfection. The results showed that the ratio of apoptotic cells was significantly reduced in tumor cells with overexpressing LIS1 in contrast to the control group. Conversely, the ratio of apoptotic cells was increased in tumor cells with knockdown of LIS1 expression (Fig. 2G and H). Therefore, the expression level of LIS1 was positively associated with the proliferation of tumor cells and negatively associated with apoptosis, indicating that LIS1 can promote tumor cell proliferation and anti-apoptosis in SACC.

LIS1 enhances migration and invasion of SACC-LM cells. As the key cellular microtubule dynein, LIS1 is highly relevant to cell movement (30,31). To identify the effect of LIS1 on the invasion and metastasis of SACC cells, wound healing assays were first used to detect horizontal cell migration. The results revealed that the migration rate of LIS1 cells was faster than that of vector cells, while that of si-LIS1 cells was markedly slower than that of si-control cells (Fig. 3A-C), and the differences were statistically significant. Moreover, the chemotactic migration and invasion abilities of SACC-LM cells were assessed using a Transwell system. As revealed in Fig. 3D-F, the number of cells that penetrated the Matrigel-coated or uncoated membrane increased following overexpression of LIS1 and decreased after knockdown of LIS1 expression in SACC-LM cells.

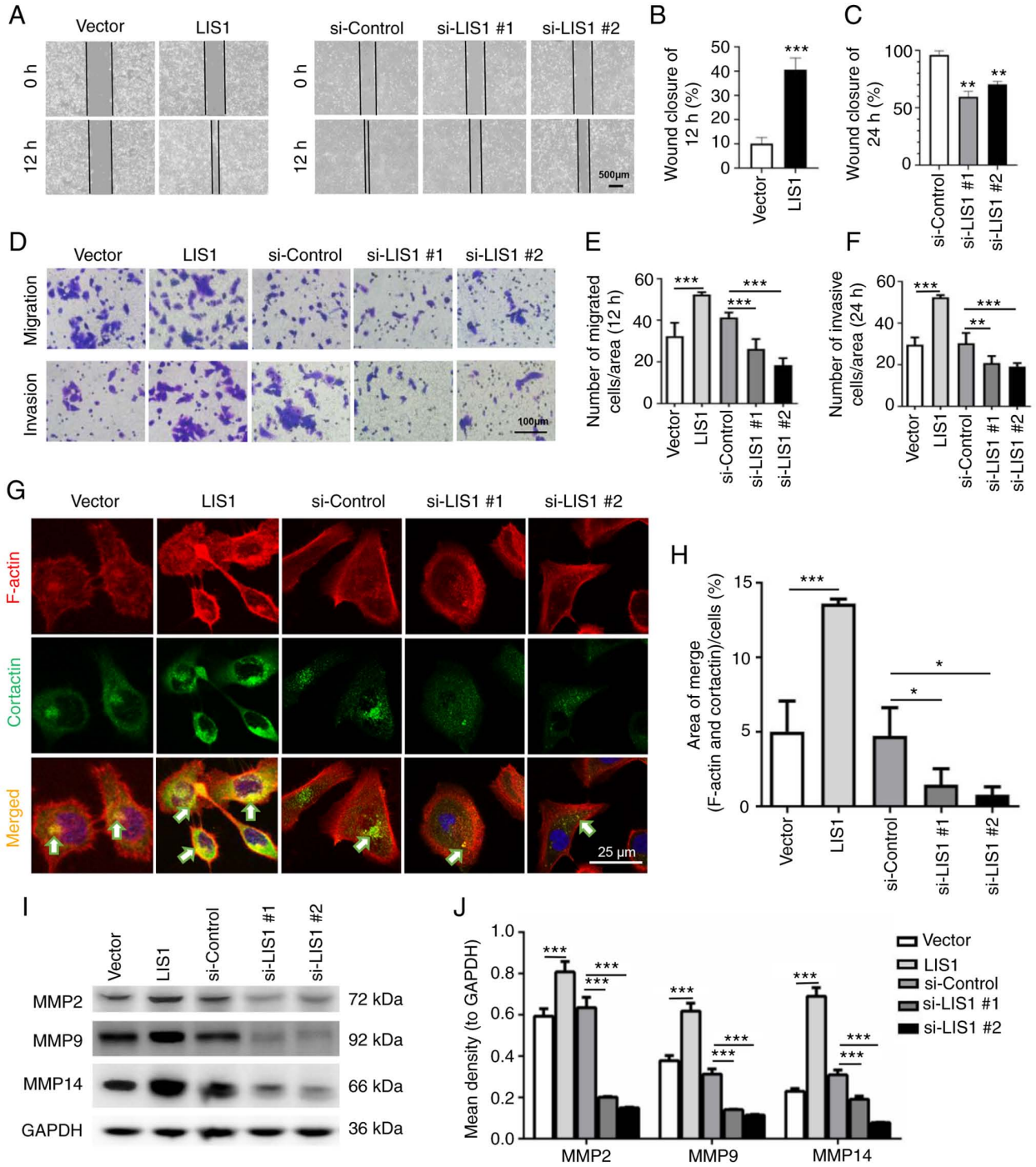

Figure 3. LIS1 promotes the migration and invasion of SACC-LM cells. (A) Wound healing assays were used to test the horizontal migration ability of SACC-LM cells with overexpressed (12 h after scratching) or knocked down (24 h after scratching) LIS1 expression. Scale bar, 500 μm. (B and C) The wound closure area of cells following (B) LIS1 overexpression and (C) LIS1 knockdown was quantitatively analyzed. (D) The effect of LIS1 overexpression and knockdown on chemotactic migration and invasion of SACC-LM cells was assessed using Transwell chambers. For migration, cells were seeded in the upper chambers for 12 h. For invasion, cells were seeded in the upper chambers coated with Matrigel for 24 h. Scale bar, 100 μm. (E and F) Quantitative statistical analysis of the number of penetrated cells after (E) 12 h of migration and (F) 24 h of invasion. (G) IF double staining of cortactin and F-actin was performed to detect invadopodia in SACC-LM cells after transfection with the LIS1 plasmid or si-LIS1. F-actin was conjugated with Alexa Fluor 568, cortactin was conjugated with Alexa Fluor 488, and the merged images (yellow) show colocalization of F-actin (red) and cortactin (green) indicating invadopodia formation. Scale bar, 25 μm. (H) Quantitative data of the area of invadopodia per cell determined by colocalization of cortactin and F-actin. (I) MMP2, MMP9, and MMP14 protein expression in SACC-LM cells with overexpressed or knocked down LIS1 expression was assessed via western blotting. (J) Quantitative analysis of MMP protein expression. Mean ± SEM; *P<0.05, **P<0.01 and ***P<0.001. LIS1, lissencephaly 1; SACC, salivary gland adenoid cystic carcinoma; si-, small interfering RNA; MMP, matrix metalloproteinase.

MMPs are enzymes that can degrade the components of the extracellular matrix (ECM). Studies have demonstrated that MMP2 and MMP9 are secreted into the extracellular space via invadopodia (32). MMP14 is usually located on the surface of the invadopodia of tumor cells, degrades the ECM and is required for the activation of MMP2 and MMP9 (33).

Therefore, the formation of invadopodia is an important factor that promotes tumor cell migration and invasion. Next, through double IF staining, it was observed whether LIS1 could regulate invadopodia in SACC-LM cells. As revealed in Fig. 3G, colocalization of cortactin and F-actin was considered to indicate the presence of invadopodia in SACC-LM. The results revealed that the number of invadopodia in LIS1-overexpressed cells was significantly increased and that in LIS1-knockdown cells it was decreased compared with the relative control groups. Quantitative analysis of the invadopodia-positive area/cells further confirmed that LIS1 promoted the formation of invadopodia in SACC-LM cells (Fig. 3H). The expression levels of MMPs was then detected via western blotting. As expected, LIS1 markedly enhanced the expression of MMP2, MMP9 and MMP14. The expression of MMP14 in the LIS1 overexpression group was nearly double that in the vector group. By contrast, the levels of MMPs were suppressed when the expression of LIS1 was knocked down in SACC-LM cells (Fig. 3I and J). These results indicated that LIS1 may regulate the migration and invasion of tumor cells by mediating the formation of invadopodia in SACC.

LIS1 promotes tumor growth in a xenograft mouse model of SACC. To corroborate the role of LIS1 in the promotion of tumor cells *in vivo*, SACC xenograft models were established via subcutaneous injection of SACC-LM cells in nude mice (Fig. 4A). LIS1 overexpression and knockdown stably transfected cell lines were primarily constructed with green fluorescent protein via recombinant lentiviruses. The overexpression and knockdown efficiencies of the stable cell lines are presented in Fig. S2. Following injection in the xenograft models, the tumor volumes and mouse weights were measured every other day (Fig. 4C). The tumor growth curve began to exhibit different trends at approximately 15 days after injection. The xenografts with LIS1-overexpressing cells grew faster than those with vector cells. Subsequently, one month later, the mice were euthanized, and the tumors were completely isolated. As revealed in Fig. 4B, the tumor volumes with high LIS1 expression were larger than those with low LIS1 expression. Next, the xenografts were weighed and statistically analyzed, and the results further indicated that the weight of tumors in the LIS1-overexpressed group was approximately 1.5 times that in the vector group, while the weight of tumors in the sh-control group was almost twice that in the sh-LIS1 group (Fig. 4D). Moreover, TUNEL assays and Ki67 immunohistochemical staining were performed to detect the tumor tissue sections. The results of the TUNEL assay demonstrated that knockdown of LIS1 significantly induced tumor cell apoptosis *in vivo*, and the number of apoptotic tumor cells was approximately 5 times that in the sh-control group. Compared with the vector group, the number of Ki67-positive cells was significantly increased in the LIS1 overexpression group (Fig. 4E-G). Collectively, the *in vivo* results demonstrated that LIS1 promoted the proliferation and inhibited the apoptosis of SACC cells, which was consistent with the *in vitro* results.

LIS1 enhances the metastatic potential of SACC cells in vivo. To further clarify whether LIS1 can promote the metastasis of SACC cells *in vivo*, a SACC metastasis model was constructed using mice. Following injection of SACC-LM cells into nude mice via the tail vein, the survival rate of the mice was continuously monitored for two months. The results showed that the mortality of mice in the LIS1 overexpression group was the highest, and this was the first experimental group with the death of a mouse. In the LIS1 overexpression group, the first mouse succumbed at approximately one month after injection, and the mouse mortality was as high as 80% at two months. Among the four groups, the survival rate was the highest in the sh-LIS1 group, and the first mouse death occurred approximately one and a half months after injection (Fig. 5A). Therefore, the survival curve revealed that reducing the level of LIS1 in SACC cells significantly prolonged the life of mice with metastatic SACC. Because the constructed stable cell line exhibited green fluorescence, live animal imaging was performed one month after the injection to observe the metastasis of tumor cells in each group. As shown in Fig. 5B, after tail vein injection of SACC-LM cells, the tumor cells mainly metastasized to the lungs of mice. The fluorescence intensity in the LIS1 overexpression group was significantly stronger than that in the vector group, while the fluorescence intensity in the sh-LIS1 group was significantly weaker than that in the sh-control group. A total of two months after establishment of the model, the lung tissue of mice was completely isolated for observation. As revealed in Fig. 5C, in the LIS1 overexpression group, numerous metastatic and necrotic areas were found in the lungs, and the number of metastatic nodules in the lungs was the highest. The morphology of the lung lobes was destroyed, and the color of the lungs was gray. In the sh-LIS1 group, the number of lung metastases was decreased compared with the sh-control group, and the morphology and color of the lungs were normal.

After embedding and sectioning, hematoxylin and eosin (H&E) and Pan-CK IHC staining of mouse lung tissue was performed. Compared with the vector group, the tumor cells in the LIS1 overexpression group exhibited severe lung metastasis, forming multiple large cancer nests. Compared with the sh-control group, the cancer nests in lung tissue in the sh-LIS1 group were rare, and the pulmonary alveolar structure was normal (Fig. 5D and E). Next, the expression of MMPs in mouse lung tissues was detected via IHC staining. As revealed in Fig. 5F and G, the levels of MMP2, MMP9 and MMP14 in the LIS1 overexpression group were higher than those in the vector group, while the levels of MMP2, MMP9 and MMP14 in the sh-LIS1 group were lower than those in the sh-control group, and the differences were significant. These results indicated that LIS1 significantly regulated the expression of MMPs and promoted lung metastasis of SACC tumor cells *in vivo*.

LIS1 interacts with CLIP-170 to regulate the proliferation and apoptosis of SACC cells through the Cdc42 signaling pathway. Cdc42 is a well-known member of the Ras homolog (Rho) family. It regulates crucial cellular processes, including the cell cycle, and cell cytoskeleton organization (34). To investigate whether LIS1 can regulate the Cdc42 pathway, the expression of Cdc42 in SACC cells was assessed using western blotting. The results revealed that the expression of LIS1 was positively associated with Cdc42 in SACC-LM cells (Fig. 6A). Following overexpression of LIS1, the inhibitor of Cdc42 was added in SACC-LM cells. The results of the CCK-8 assay revealed that the proliferation

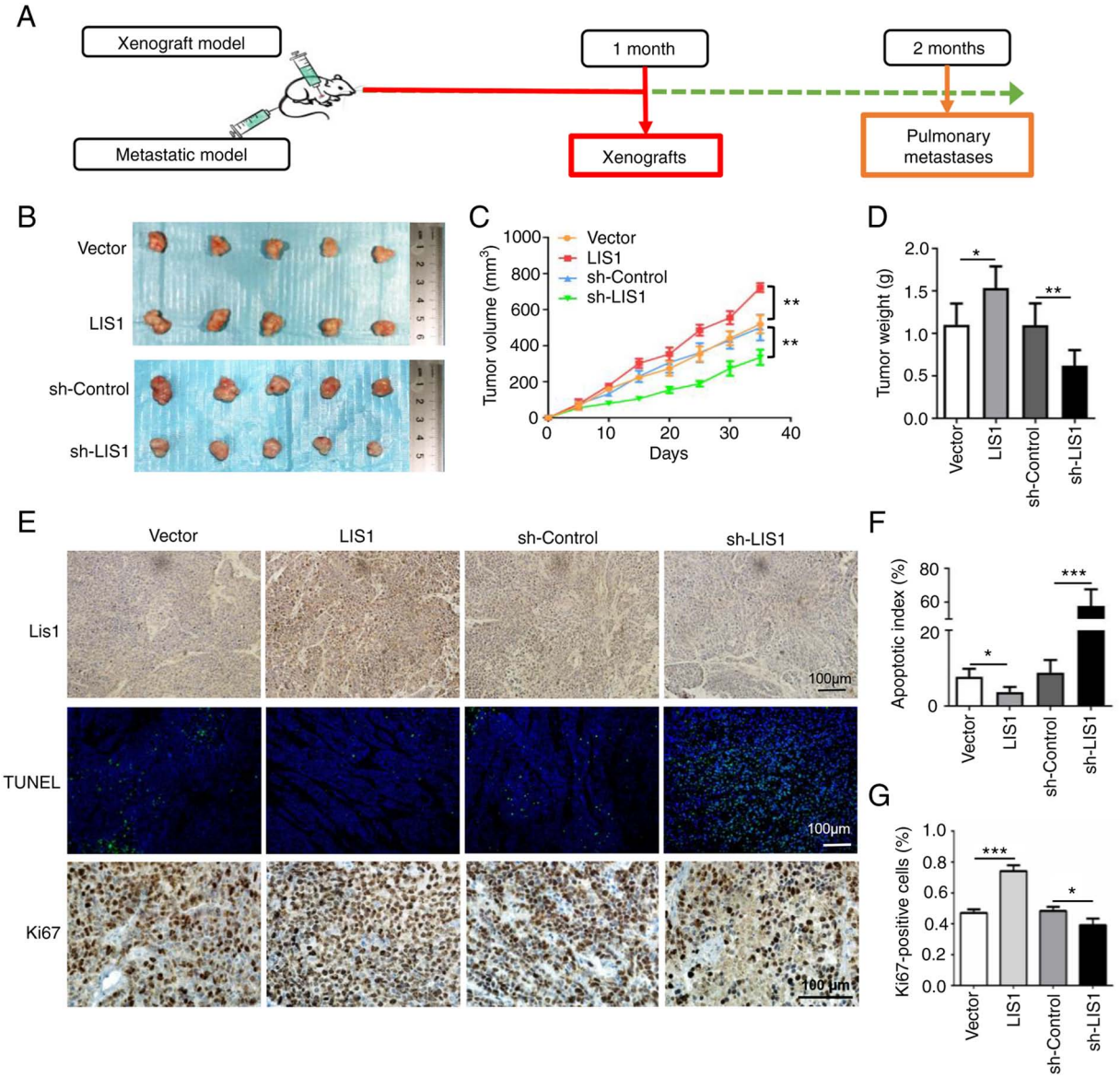

Figure 4. LIS1 enhances tumor growth in a SACC xenograft mouse model. (A) Schematic representation of the animal model establishment. A total of 40 nude mice were randomly divided into two sections, one for nude mouse xenograft tumors and the other for metastasis models. For xenograft models, $1x10^7$ cells in 100 μl PBS were subcutaneously injected into the right flank of mice (n=5 per group). Subsequently, one month later, the xenograft tumors were removed. (B) Images of xenograft tumors harvested from nude mice following injection of tumor cells (vector, LIS1 overexpression, sh-Control and sh-LIS1 cells). (C) The volume of xenograft tumors was measured every five days, and the changes in the tumor weight of mice wered recorded. (D) The weight of xenograft tumors was measured when the xenografts were removed 35 days after injection of the tumor cells. (E) A TUNEL assay was performed to assess cell apoptosis in the tumor tissues, and the expression of Ki67 in xenograft tumors was detected by immunohistochemistry. Scale bar, 100 μm. (F) Quantitative statistical analysis of TUNEL assay results. (G) Quantitative statistics for the percentage of Ki67-positive cells. Mean ± SEM; *P<0.05, **P<0.01 and ***P<0.001. LIS1, lissencephaly 1; SACC, salivary gland adenoid cystic carcinoma; PBS, phosphate-buffered saline; sh-, short hairpin RNA; TUNEL, terminal deoxynucleotidyl transferase dUTP nick-end labeling.

ability of tumor cells was significantly decreased compared with the LIS1 overexpression group, indicating that Cdc42 may be a pivotal downstream factor of LIS1 in SACC-LM cells (Fig. 6B). Studies have shown that the WD-40 repeat domain of the LIS1 protein can interact with the second zinc finger motif at the COOH-terminus of CLIP170 to regulate the dynamic balance of microtubules and microfilaments, thus playing an essential role in cell division and cell migration (13,16). To verify whether LIS1 and CLIP170 can interact with each other in SACC-LM cells, Co-IP was performed. When LIS1 was overexpressed in SACC-LM cells, the level of CLIP170 expressed with IP-LIS1 was significantly higher than that in the vector group, and vice versa, indicating that LIS1 and CLIP170 could bind together in SACC-LM cells (Fig. 6C). Next, the siRNA-CLIP170 sequence was used to knock down CLIP170 in SACC-LM cells (Fig. S1E and F). Using CCK-8 and TUNEL assays, when the expression of CLIP170 was knocked down after overexpression of LIS1, the proliferation of tumor cells was significantly decreased, and the apoptosis of tumor cells was increased compared with the LIS1 overexpression group. Interestingly, when Cdc42 inhibitor was added in SACC-LM cells with double-transfection of LIS1 and si-CLIP170, the proliferation of cells was not significantly inhibited, and the apoptosis level was also not increased compared with the LIS1 and si-CLIP170

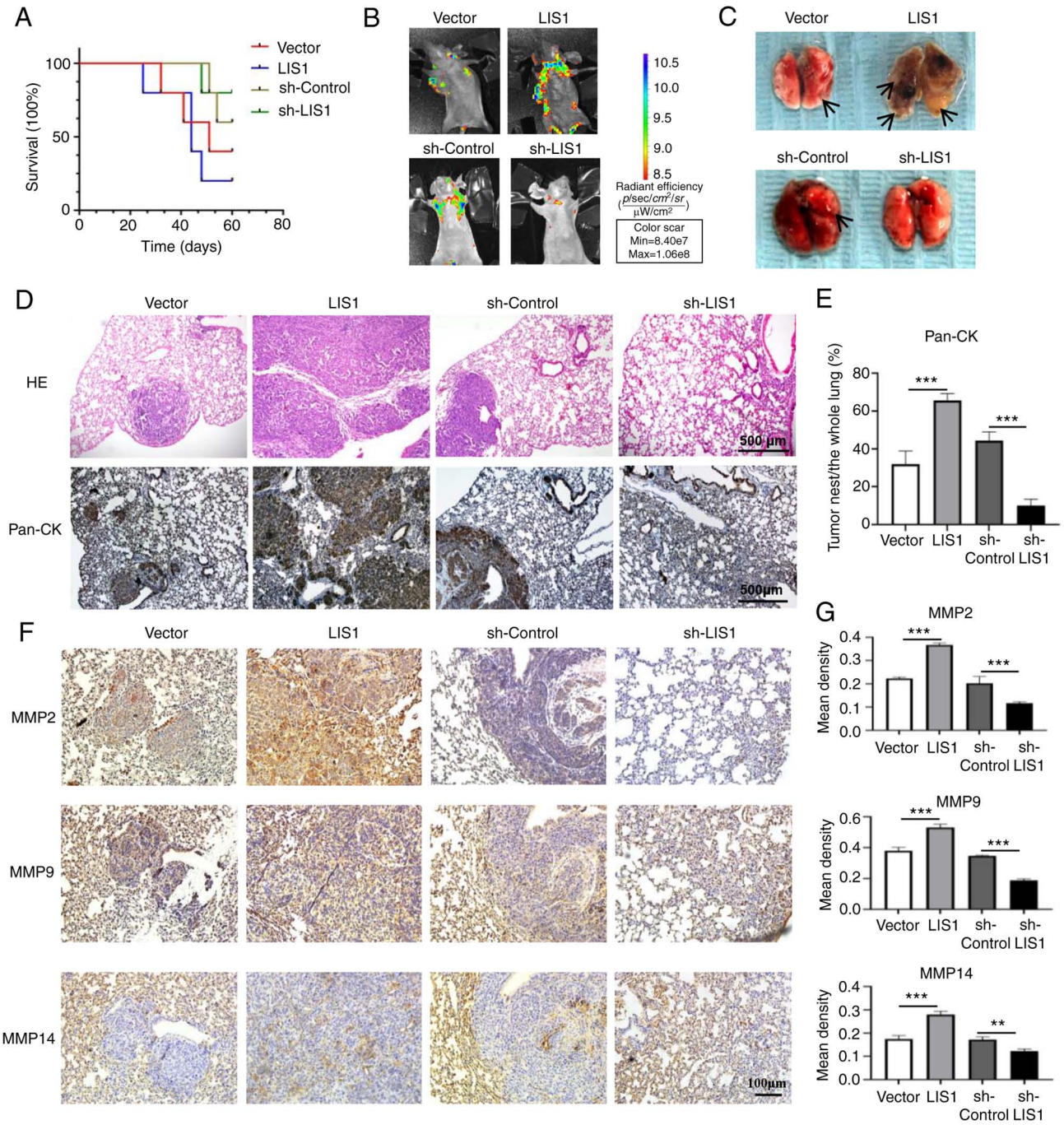

Figure 5. LIS1 enhances tumor metastasis in a SACC metastasis nude mouse model. For the metastatic models, $5x10^6$ cells in 100 μl PBS were injected into the nude mice via the tail vein (n=5 per group). (A) Kaplan-Meier survival curve of the mice after injection of LIS1 overexpression or knockdown SACC cells via the tail vein. (B) The Living Image system was used to observe metastasis 30 days after intravenous injection of tumor cells. (C) Representative images of the lungs isolated from metastatic nude mice. (D) The lungs from SACC-LM metastatic model mice were stained with H&E, and immunohistochemical staining to detect Pan-CK was performed. Scale bar, 500 μm. (E) Quantitative analysis of the percentage of tumor area in the whole lung tissue according to immunohistochemical staining of Pan-CK. (F) The expression levels of MMP2, MMP9, and MMP14 in the lungs of the SACC-LM metastatic model mice were detected by immunohistochemical staining. (G) Quantitative analysis of immunohistochemical staining of MMPs. Scale bar, 100 μm. Mean ± SEM; **P<0.01 and ***P<0.001. LIS1, lissencephaly 1; SACC, salivary gland adenoid cystic carcinoma; PBS, phosphate-buffered saline; H&E, hematoxylin and eosin; MMP, matrix metalloproteinase; sh-, short hairpin RNA.

double-transfected group, suggesting that LIS1 needs to interact with CLIP170 to activate Cdc42, so as to enhance the proliferation and anti-apoptosis ability of tumor cells (Fig. 6D-F). Moreover, the expression levels of the proliferation-related gene cyclin D1 and the apoptosis-related gene BCL2 were further detected via western blotting (Fig. 6G and H). Overexpression of LIS1 in SACC cells upregulated cyclin D1 and BCL2, while knockdown of CLIP170 after overexpression of LIS1 in tumor cells significantly reduced the levels of cyclin D1 and BCL2. However, compared with the LIS1 and si-CLIP170 double-transfection group, the expression of cyclin D1 and BCL2 in tumor cells was not significantly decreased in the LIS1 + si-CLIP170 + ML141 group. These results demonstrated that LIS1 interacted with CLIP170 to form the LIS1/CLIP170 protein complex, which

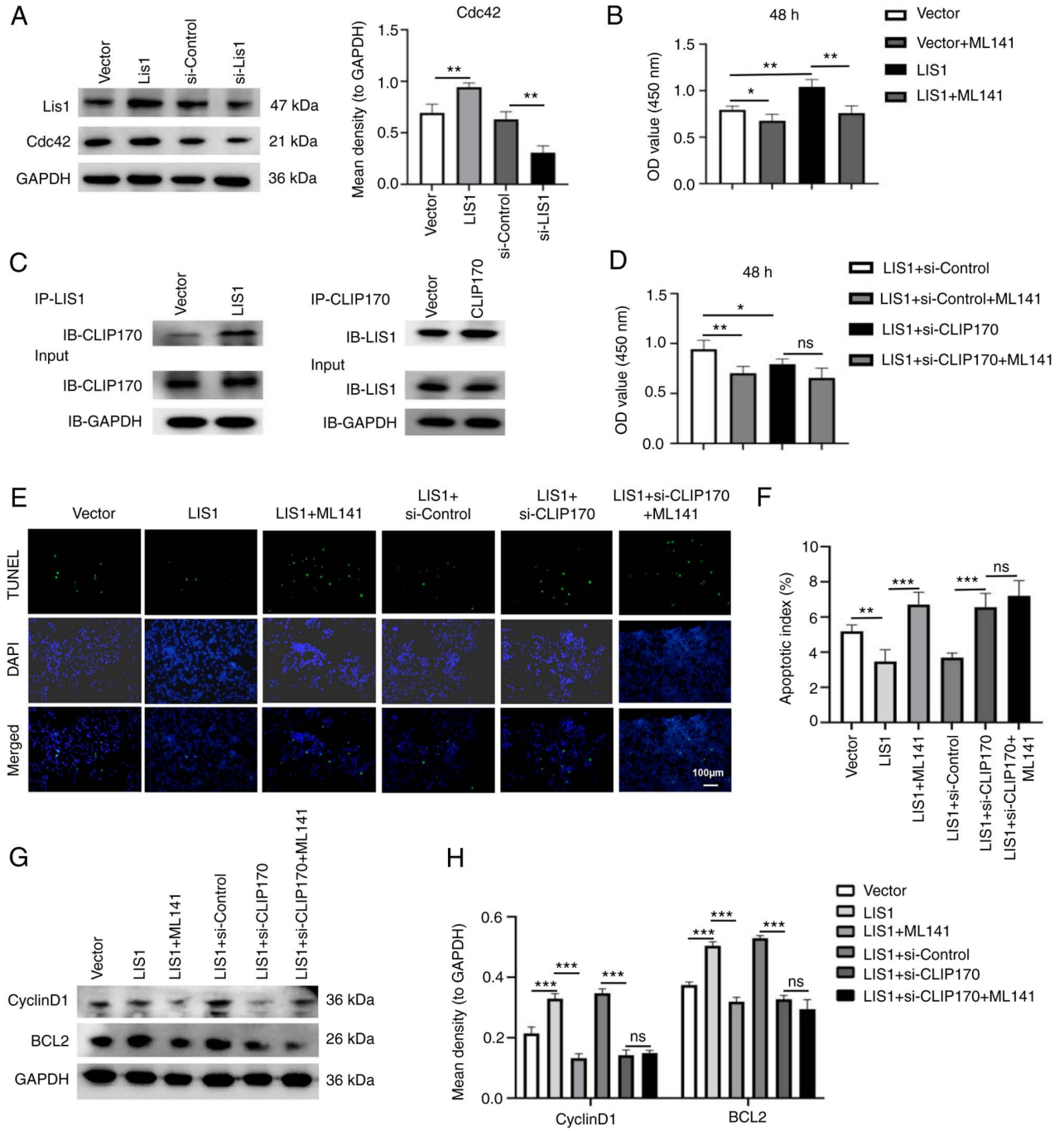

Figure 6. Protein complex LIS1/CLIP170 regulates SACC-LM cell proliferation and apoptosis through the Cdc42 pathway. (A) The protein level of LIS1 was detected by western blotting and statistically analyzed. (B) The proliferation of tumor cells treated with ML141 (Cdc42 inhibitor) was assessed by CCK-8 assay. (C) Cells were transfected with LIS1 or CLIP170. Immunoprecipitation was then performed to examine the interaction between LIS1 and endogenous CLIP170. (D) SACC-LM cells were transfected with vector or LIS1 and then transfected with si-control or si-CLIP170. The proliferation of tumor cells with or without the treatment of ML141 was assessed by CCK-8 assay. (E) TUNEL assays were performed to examine cell apoptosis. (F) Quantitative statistical analysis of TUNEL assay results. (G) Cyclin D1 and BCL2 protein expression was assessed via western blotting in SACC-LM cells. (H) Quantitative analysis of the protein level in G. Mean ± SEM; *P<0.05, **P<0.01 and ***P<0.001. LIS1, lissencephaly 1; CLIP170, cytoplasmic linker protein 170; SACC, salivary gland adenoid cystic carcinoma; Cdc42, cell division control protein 42 homolog; CCK-8, Cell Counting Kit-8; si-, small interfering RNA; TUNEL, terminal deoxynucleotidyl transferase dUTP nick-end labeling; IP, immunoprecipitation.

could activate the Cdc42 signaling pathway to promote the proliferation and anti-apoptosis of SACC cells.

LIS1 interacts with CLIP170 to modulate metastasis of SACC cells through the Cdc42 signaling pathway. Numerous studies have demonstrated that Cdc42 is closely related to cell migration. Cao *et al* (35) revealed that Cdc42 regulates the invasive ability of breast cancer cells by regulating the formation of lamellipodia and expression of MMPs. First, wound healing and Transwell assays were used to verify whether the LIS1/CLIP170 complex could regulate the migration and invasion of SACC cells via the Cdc42 pathway. The results revealed that compared with the LIS1 overexpression group, knockdown of CLIP170 after overexpression of LIS1 in SACC cells significantly reduced the

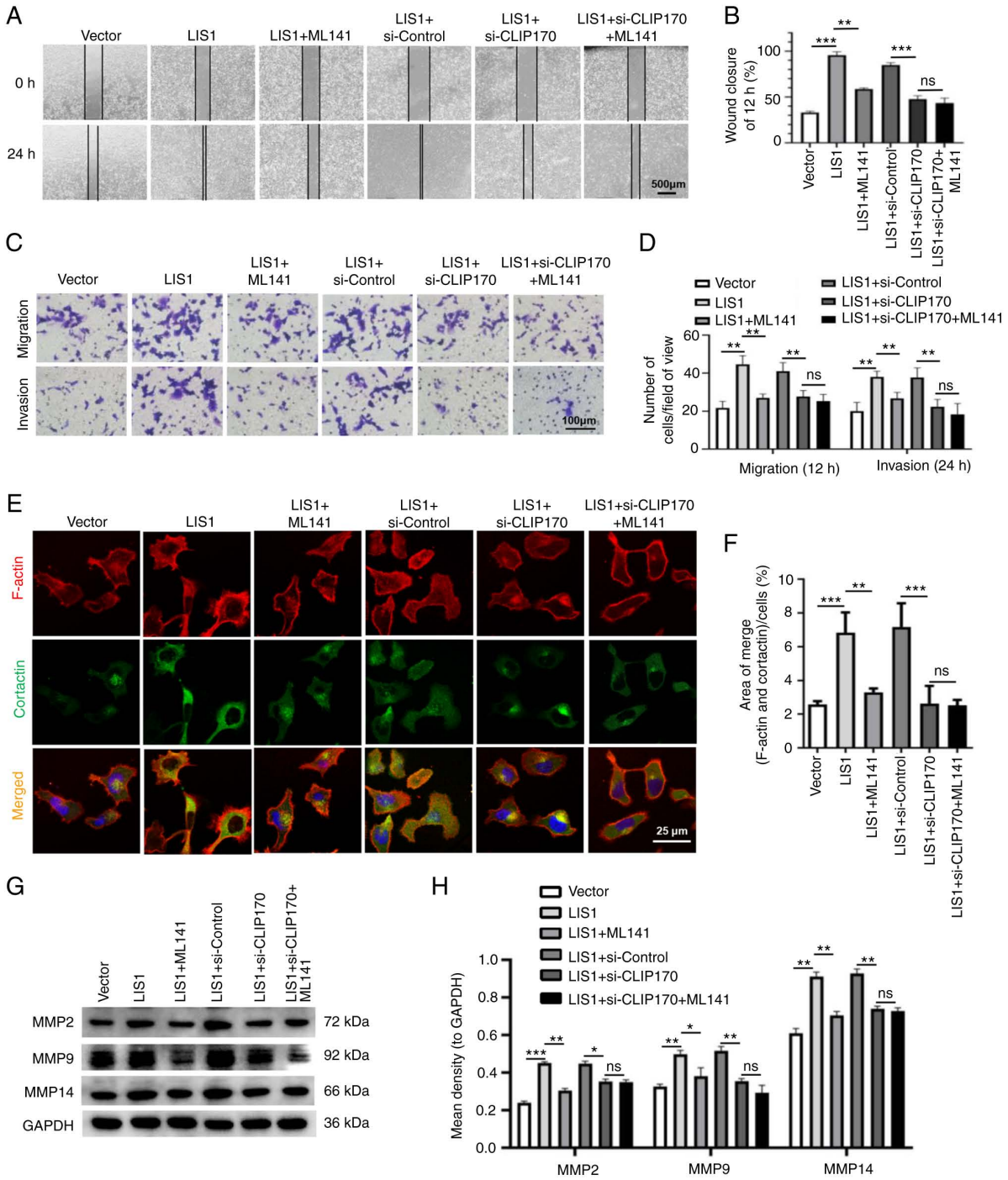

Figure 7. Protein complex LIS1/CLIP170 regulates SACC-LM cell migration and invasion through the Cdc42 signaling pathway. Tumor cells were transfected with vector or LIS1 and then transfected with si-control or si-CLIP170, and ML141, as an inhibitor of Cdc42, was added into SACC-LM cells. (A) Wound healing assays were performed to assess the horizontal migration ability of SACC-LM cells. Scale bar, 500 μm. (B) Quantitative statistical analysis of the wound healing assay results. (C) The chemotactic migration and Matrigel invasion of SACC-LM cells were measured using Transwell assays. Scale bar, 100 μm. (D) Quantitative analysis of the migrated cells at 12 h and the cells that invaded through the Matrigel membrane at 24 h. (E) Invadopodia formation in SACC-LM cells was detected by IF double staining. The merged images (yellow) show the colocalization of cortactin (green) and F-actin (red). Scale bar, 25 μm. (F) Quantitative statistics of the area of invadopodia per cell determined by the colocalization of cortactin and F-actin. (G) MMP2, MMP9, and MMP14 protein levels in SACC-LM cells were measured via western blotting. (H) Quantitative analysis of MMP protein levels. Mean ± SEM; *P<0.05, **P<0.01 and ***P<0.001. LIS1, lissencephaly 1; CLIP170, cytoplasmic linker protein 170; SACC, salivary gland adenoid cystic carcinoma; Cdc42, cell division control protein 42 homolog; MMP, matrix metalloproteinase; si-, small interfering RNA; ns, not significant.

migration and invasion of tumor cells, while the Cdc42 inhibitor could not significantly decrease the migration and invasion of tumor cells in the double-transfection of LIS1 and si-CLIP170 group (Fig. 7A-D). In addition, through double IF staining, changes in the formation of invadopodia were detected in SACC cells after treatment. The results showed that when CLIP170 was knocked down after overexpression of LIS1, the number of invadopodia formed by tumor cells was significantly reduced. Concurrently, it was determined that the number of invadopodia in LIS1 + si-CLIP170 + ML141 group was not less than that in

the LIS1 + si-CLIP170 group (Fig. 7E and F). Moreover, the expression of MMP proteins was assessed via western blotting, and the results were consistent with the aforementioned results (Fig. 7G and H). Therefore, these results demonstrated that LIS1 may interact with CLIP170 to form the LIS1/CLIP170 protein complex and then activate Cdc42 to regulate the expression of MMPs by regulating the formation of invadopodia in SACC cells, thus promoting degradation of the ECM to enhance metastasis.

Discussion

Several studies have revealed that LIS1 is a key node protein that participates in several pathways, including association with the molecular motor cytoplasmic dynein, the reelin signaling pathway, and the platelet-activating factor pathway (11,12,36). Recently, the role of LIS1 in tumors has begun to attract attention. A previous study revealed that LIS1 can positively regulate the migration and invasion of neuroblastoma and glioma (37). In non-neurological tumors, the expression level of LIS1 was also revealed to be upregulated and promote the proliferation and metastasis of tumor cells (11). In SACC, there are three histological patterns (cribriform, tubular, and solid). One of the important prognostic factors of SACC is the percentage of solid tumor components. The larger the percentage of solid tumors, the lower the 15-year survival rate of patients with SACC (38). In the present study, it was demonstrated that LIS1 was highly expressed in SACC tissues. Among the three subtypes of SACC, the level of LIS1 was the highest in the solid type with low differentiation. In addition, LIS1 expression was significantly upregulated in metastatic SACC compared with non-metastatic SACC. Therefore, these clinical results indicated that LIS1 plays a critical role in the malignant progression of SACC, suggesting that LIS1 may be a potential therapeutic target.

LIS1 is part of a complex that interacts with diverse cortical factors and centrosomal proteins at kinetochores on chromosomes, mitotic spindles and the cell cortex, and has been implicated in regulation of mitotic spindles and chromosome segregation during mitosis (39,40). There is a close correlation between LIS1 and cancer stem cells (CSCs). The main characteristics of CSCs are relatively unlimited division and proliferation, multidirectional differentiation potential and self-renewal ability (41). Brehar *et al* (42) revealed that the expression of the *LIS1* gene in CD133-positive glioblastoma cells was 60 times higher than that in CD133-negative glioblastoma cells. In addition, Wang *et al* (43) reported that LIS1 promoted endogenous stem cell regeneration in submandibular salivary glands, and this process was mainly actioned through the interaction of LIS1 and stem cell markers (SOX2 and Sca-1). The results of the present study indicated that overexpression of LIS1 significantly enhanced the proliferation and inhibited the apoptosis of SACC-LM cells *in vitro* and *in vivo*, while knockdown of LIS1 expression decreased the proliferation of tumor cells and increased the level of apoptosis. Therefore, LIS1 may control cell division and cell cycle progression by modulating mitotic spindle assembly or stem cell gene expression, thereby regulating the proliferation and apoptosis of tumor cells; the specific mechanism in SACC needs to be further studied.

Another biological feature of malignant tumors is high recurrence and metastasis rates. In a previous study of 130 cases of SACC, the recurrence rate was 43.8% and the distant metastasis rate was 28.5%, which is the main cause for the poor prognosis of patients with SACC (44). Acting as a microtubule-associated protein, *LIS1* was the first gene related to neuronal migration disorders that was cloned in humans (45). LIS1 regulates leading edge dynein, potentially serving as a holdfast for microtubules that invade the actin-network at the front of the cell and thus regulating the formation of lamellipodial protrusions (46). In the process of tumor metastasis, cancer cells must migrate into the ECM and infiltrate the blood and lymphatic vessels (32). MMPs are critical proteases that degrade the ECM and thus the most important enzyme system in regulating the dynamic balance of the ECM. The main MMP family is located in the invadopodia of cancer cells (33). Therefore, the formation of invadopodia plays an essential role in degradation of the ECM. In the present study, *in vitro* experiments were first performed to verify that LIS1 could promote the migration and invasion abilities of SACC-LM cells. Through double fluorescence staining, it was determined that LIS1 could regulate the formation of invadopodia and was positively correlated with the expression of MMPs, which suggests that LIS1 may promote SACC invasion and metastasis through ECM degradation mediated by the formation of invadopodia in tumor cells. It was further verified *in vivo* that overexpression of LIS1 significantly promoted lung metastasis of SACC, while knockdown of LIS1 significantly inhibited tumor metastasis and prolonged the life of mice. The *in vivo* results provide strong evidence of the effectiveness and feasibility of targeting LIS1 in the treatment of SACC. Prior literature has focused on the involvement of the MYB pathway in the ACC mutational landscape, and there is significant evidence for its role in ACC tumorigenesis (47,48). A previous study reported that a protein complex composed of the basic helix-loop-helix (bHLH) associated with MYB transcription factors and the WD40 repeat protein initiates multiple cellular differentiation pathways (49). LIS1 is a WD40 repeat scaffold protein, which interacts with components of the cytoplasmic dynein motor complex to regulate dynein-dependent cell motility (41,50). Therefore, whether LIS1 interacts with MYB to participate in the malignant progression of SACC needs further study. It has been demonstrated that LIS1 and CLIP170 colocalize at kinetochores and tips of astral microtubules in interphase cells, nuclei of prophase cells, and cortical sites contacting astral microtubules in mitotic cells (13). In addition, a previous study indicated that Cdc2-mediated phosphorylation of CLIP170 was important for its localization at microtubule-plus ends in the G2 phase and during G2/M transition, which is related to CLIP170 function during cell cycle progression (20). CLIP170 depletion led to centrosome reduplication after the S phase, suggesting that CLIP170 may be a factor that controls cell mitosis by regulating the number of centrosomes (20). The results of the present study provided evidence that LIS1 and CLIP170 could form a protein complex in SACC-LM cells. Furthermore, it was determined that the expression of LIS1 was positively associated with the level of Cdc42, and LIS1 could regulate the proliferation of SACC-LM cells through activation of the Cdc42 pathway. Interestingly, the results demonstrated that inhibition of Cdc42 in SACC-LM cells double-transfected with LIS1 and si-CLIP170 hardly reduced the proliferation and anti-apoptosis of tumor cells, suggesting that the interaction between LIS1 and CLIP170 may coordinate the tumor cell cycle, and then promote the proliferation and

anti-apoptosis of SACC cells via the Cdc42 signaling pathway. Moreover, when the expression of CLIP170 was knocked down after overexpression of LIS1, it was determined that the invasion and migration ability of SACC-LM cells treated with Cdc42 inhibitor was not significantly suppressed, indicating that the activation of Cdc42 by LIS1 in promoting tumor cell invasion and metastasis was also regulated through its interaction with CLIP170. A previous study revealed that the formation of the lamellipodia necessary for cell invasion is regulated by Cdc42, while CLIP170 can form a complex with Rac1/Cdc42, IQGAP1 and kinesin, which regulates the invasion ability of breast cancer cells by mediating the formation of invadopodia (51). The activation of Cdc42 participates in invadopodia structures and is responsible for the production or activation of MMPs (17,52,53). In the present study, it was revealed that the interaction between LIS1 and CLIP170 regulated the formation of invadopodia and degradation of the ECM through activation of the Cdc42 signaling pathway, leading to promotion of SACC cell invasion and metastasis. In a following study, the signaling pathway of LIS1/CLIP170/Cdc42 will be further verified in clinical samples and the specific mechanism by which Cdc42 regulates the malignant progression of SACC will be explored.

In conclusion, the *in vivo* and *in vitro* experimental results demonstrated that LIS1 promoted tumor cell proliferation, inhibited tumor cell apoptosis and increased SACC invasion and metastatic abilities. Concurrently, it was also revealed that LIS1 interacts with CLIP170 to form a protein complex, which regulates tumor cell division and the formation of invadopodia via the Cdc42 signaling pathway. It is suggested that LIS1/CLIP170 may coordinate the polymerization and dynamic balance of microtubules by activation of the small Rho GTPase Cdc42, thus promoting proliferation and metastasis. The data of the present study provide a novel mechanism underlying the malignant development of tumors and suggest LIS1/CLIP170/Cdc42 as a new therapeutic target for treatment of SACC.

Acknowledgements

Not applicable.

Funding

The present study was supported by grants from the Natural Science Foundation of China (grant no. 81802706 to LG; and grant no. 81771032 to FW), the Scientific Foundation of the Department of Education of Liaoning Province (grant no. LZ2020035 to LG), and the Natural Science Foundation of Liaoning Province (grant no. 2021-MS-293 to LG).

Availability of data and materials

Publicly available datasets analyzed in the present study can be found at NCBI GenBank (Accession number: NM_000430; NM_198240). All data generated or analyzed during this study are included in this published article.

Authors' contributions

LL, ZW and NK performed all the experiments and contributed to the collection of data. JL, DJ and LW contributed to data analysis and interpretation. NK, DJ and LW were involved in useful discussions and revised the manuscript. FW contributed to partial conception and design, data analysis and interpretation, and drafting of the manuscript. LG contributed to conception and design, data analysis and interpretation, as well as drafting and editing of the manuscript. LG and FW confirm the authenticity of all the raw data. All authors read and approved the final manuscript.

Ethics approval and consent to participate

The procedures of the present study concerning human subjects were approved (approval no. DY2021-005) by the Medical Ethics Committee of Dalian Medical University (Dalian, China). Written informed consent was obtained from all patients after detailed explanation of the procedure and the intended use of the tissues. The animal experiments were approved (approval no. AEE20017) by the Animal Experimental Ethics Committee of Dalian Medical University. All experiments were performed according to standard protocols, in compliance with the Guide of the Ethics Committee of Dalian Medical University and were conducted following the Declaration of Helsinki.

Patient consent for publication

Not applicable.

Competing interests

The authors declare that they have no competing interests.

References

1. Laurie SA, Ho AL, Fury MG, Sherman E and Pfister DG: Systemic therapy in the management of metastatic or locally recurrent adenoid cystic carcinoma of the salivary glands: A systematic review. Lancet Oncol 12: 815-824, 2011.
2. Su BH, Qu J, Song M, Huang XY, Hu XM, Xie J, Zhao Y, Ding LC, She L, Chen J, *et al*: NOTCH1 signaling contributes to cell growth, anti-apoptosis and metastasis in salivary adenoid cystic carcinoma. Oncotarget 5: 6885-6895, 2014.
3. Kong J, Tian H, Zhang F, Zhang Z, Li J, Liu X, Li X, Liu J, Li X, Jin D, *et al*: Extracellular vesicles of carcinoma-associated fibroblasts creates a pre-metastatic niche in the lung through activating fibroblasts. Mol Cancer 18: 175, 2019.
4. Al Absi A, Wurzer H, Guerin C, Hoffmann C, Moreau F, Mao X, Brown-Clay J, Petrolli R, Casellas CP, Dieterle M, *et al*: Actin cytoskeleton remodeling drives breast cancer cell escape from natural killer-mediated cytotoxicity. Cancer Res 78: 5631-5643, 2018.
5. Prahl LS, Bangasser PF, Stopfer LE, Hemmat M, White FM, Rosenfeld SS and Odde DJ: Microtubule-based control of motor-clutch system mechanics in glioma cell migration. Cell Rep 25: 2591-2604.e8, 2018.
6. Sharma P, Alsharif S, Fallatah A and Chung BM: Intermediate filaments as effectors of cancer development and metastasis: A focus on keratins, vimentin, and nestin. Cells 8: 497, 2019.
7. Jung YS, Wang W, Jun S, Zhang J, Srivastava M, Kim MJ, Lien EM, Shang J, Chen J, McCrea PD, *et al*: Deregulation of CRAD-controlled cytoskeleton initiates mucinous colorectal cancer via β-catenin. Nat Cell Biol 20: 1303-1314, 2018.
8. Peng JM, Bera R, Chiou CY, Yu MC, Chen TC, Chen CW, Wang TR, Chiang WL, Chai SP, Wei Y, *et al*: Actin cytoskeleton remodeling drives epithelial-mesenchymal transition for hepatoma invasion and metastasis in mice. Hepatology 67: 2226-2243, 2018.
9. DeSantis ME, Cianfrocco MA, Htet ZM, Tran PT, Reck-Peterson SL and Leschziner AE: Lis1 has two opposing modes of regulating cytoplasmic dynein. Cell 170: 1197-1208.e12, 2017.

10. Allanson JE, Ledbetter DH and Dobyns WB: Classical lissencephaly syndromes: Does the face reflect the brain? J Med Genet 35: 920-923, 1998.
11. Lo FY, Chen HT, Cheng HC, Hsu HS and Wang YC: Overexpression of PAFAH1B1 is associated with tumor metastasis and poor survival in non-small cell lung cancer. Lung Cancer 77: 585-592, 2012.
12. Yang R, Chen Y, Tang C, Li H, Wang B, Yan Q, Hu J and Zou S: MicroRNA-144 suppresses cholangiocarcinoma cell proliferation and invasion through targeting platelet activating factor acetylhydrolase isoform 1b. BMC Cancer 14: 917, 2014.
13. Coquelle FM, Caspi M, Cordelières FP, Dompierre JP, Dujardin DL, Koifman C, Martin P, Hoogenraad CC, Akhmanova A, Galjart N, *et al*: LIS1, CLIP-170's key to the dynein/dynactin pathway. Mol Cell Biol 22: 3089-3102, 2002.
14. Jakka P, Bhargavi B, Namani S, Murugan S, Splitter G and Radhakrishnan G: Cytoplasmic linker protein CLIP170 negatively regulates TLR4 signaling by targeting the TLR adaptor protein TIRAP. J Immunol 200: 704-714, 2018.
15. Sun X, Li D, Yang Y, Ren Y, Li J, Wang Z, Dong B, Liu M and Zhou J: Microtubule-binding protein CLIP-170 is a mediator of paclitaxel sensitivity. J Pathol 226: 666-673, 2012.
16. Gao L, Xue B, Xiang B and Liu KJ: Arsenic trioxide disturbs the LIS1/NDEL1/dynein microtubule dynamic complex by disrupting the CLIP170 zinc finger in head and neck cancer. Toxicol Appl Pharmacol 403: 115158, 2020.
17. Murphy NP, Binti Ahmad Mokhtar AM, Mott HR and Owen D: Molecular subversion of Cdc42 signalling in cancer. Biochem Soc Trans 49: 1425-1442, 2021.
18. Murphy NP, Mott HR and Owen D: Progress in the therapeutic inhibition of Cdc42 signalling. Biochem Soc Trans 49: 1443-1456, 2021.
19. Chernichenko N, Omelchenko T, Deborde S, Bakst RL, He S, Chen CH, Gusain L, Vakiani E, Katabi N, Hall A and Wong RJ: Cdc42 mediates cancer cell chemotaxis in perineural invasion. Mol Cancer Res 18: 913-925, 2020.
20. Yang X, Li H, Liu XS, Deng A and Liu X: Cdc2-mediated phosphorylation of CLIP-170 is essential for its inhibition of centrosome reduplication. J Biol Chem 284: 28775-28782, 2009.
21. Fukata M, Watanabe T, Noritake J, Nakagawa M, Yamaga M, Kuroda S, Matsuura Y, Iwamatsu A, Perez F and Kaibuchi K: Rac1 and Cdc42 capture microtubules through IQGAP1 and CLIP-170. Cell 109: 873-885, 2002.
22. Maldonado MDM and Dharmawardhane S: Targeting Rac and Cdc42 GTPases in cancer. Cancer Res 78: 3101-3111, 2018.
23. Stengel KR and Zheng Y: Essential role of Cdc42 in Ras-induced transformation revealed by gene targeting. PLoS One 7: e37317, 2012.
24. Bai J, Li L, Kou N, Bai Y, Zhang Y, Lu Y, Gao L and Wang F: Low level laser therapy promotes bone regeneration by coupling angiogenesis and osteogenesis. Stem Cell Res Ther 12: 432, 2021.
25. Gao L, Zhang W, Zhong WQ, Liu ZJ, Li HM, Yu ZL and Zhao YF: Tumor associated macrophages induce epithelial to mesenchymal transition via the EGFR/ERK1/2 pathway in head and neck squamous cell carcinoma. Oncol Rep 40: 2558-2572, 2018.
26. Livak KJ and Schmittgen TD: Analysis of relative gene expression data using real-time quantitative PCR and the 2(-Delta Delta C(T)) method. Methods 25: 402-408, 2001.
27. Zhang Y, Bai Y, Bai J, Li L, Gao L and Wang F: Targeting soluble epoxide hydrolase with TPPU alleviates irradiation-induced hyposalivation in mice via preventing apoptosis and microcirculation disturbance. Adv Ther 3: 2000115, 2020.
28. Gao L, Wang FQ, Li HM, Yang JG, Ren JG, He KF, Liu B, Zhang W and Zhao YF: CCL2/EGF positive feedback loop between cancer cells and macrophages promotes cell migration and invasion in head and neck squamous cell carcinoma. Oncotarget 7: 87037-87051, 2016.
29. Li HM, Yang JG, Liu ZJ, Wang WM, Yu ZL, Ren JG, Chen G, Zhang W and Jia J: Blockage of glycolysis by targeting PFKFB3 suppresses tumor growth and metastasis in head and neck squamous cell carcinoma. J Exp Clin Cancer Res 36: 7, 2017.
30. Markus SM, Marzo MG and McKenney RJ: New insights into the mechanism of dynein motor regulation by lissencephaly-1. Elife 9: e59737, 2020.
31. Chen W, Wang W, Sun X, Xie S, Xu X, Liu M, Yang C, Li M, Zhang W, Liu W, *et al*: NudCL2 regulates cell migration by stabilizing both myosin-9 and LIS1 with Hsp90. Cell Death Dis 11: 534, 2020.
32. Gorshtein G, Grafinger O and Coppolino MG: Targeting SNARE-mediated vesicle transport to block invadopodium-based cancer cell invasion. Front Oncol 11: 679955, 2021.
33. Seano G and Primo L: Podosomes and invadopodia: Tools to breach vascular basement membrane. Cell Cycle 14: 1370-1374, 2015.
34. Qadir MI, Parveen A and Ali M: Cdc42: Role in cancer management. Chem Biol Drug Des 86: 432-439, 2015.
35. Cao H, Eppinga RD, Razidlo GL, Krueger EW, Chen J, Qiang L and McNiven MA: Stromal fibroblasts facilitate cancer cell invasion by a novel invadopodia-independent matrix degradation process. Oncogene 35: 1099-1110, 2016.
36. Reiner O, Sapoznik S and Sapir T: Lissencephaly 1 linking to multiple diseases: Mental retardation, neurodegeneration, schizophrenia, male sterility, and more. Neuromolecular Med 8: 547-565, 2006.
37. Suzuki SO, McKenney RJ, Mawatari SY, Mizuguchi M, Mikami A, Iwaki T, Goldman JE, Canoll P and Vallee RB: Expression patterns of LIS1, dynein and their interaction partners dynactin, NudE, NudEL and NudC in human gliomas suggest roles in invasion and proliferation. Acta Neuropathol 113: 591-599, 2007.
38. Perzin KH, Gullane P and Clairmont AC: Adenoid cystic carcinomas arising in salivary glands: A correlation of histologic features and clinical course. Cancer 42: 265-282, 1978.
39. Yingling J, Youn YH, Darling D, Toyo-Oka K, Pramparo T, Hirotsune S and Wynshaw-Boris A: Neuroepithelial stem cell proliferation requires LIS1 for precise spindle orientation and symmetric division. Cell 132: 474-486, 2008.
40. Moon HM, Youn YH, Pemble H, Yingling J, Wittmann T and Wynshaw-Boris A: LIS1 controls mitosis and mitotic spindle organization via the LIS1-NDEL1-dynein complex. Hum Mol Genet 23: 449-466, 2014.
41. Brehar FM, Dragomir MP, Petrescu GED and Gorgan RM: Fighting cancer stem cell fate by targeting LIS1 a WD40 repeat protein. Front Oncol 9: 1142, 2019.
42. Brehar FM, Gafencu AV, Trusca VG, Fuior EV, Arsene D, Amaireh M, Giovani A and Gorgan MR: Preferential association of lissencephaly-1 gene expression with $CD133^+$ glioblastoma cells. J Cancer 8: 1284-1291, 2017.
43. Wang XY, Yu J, Zhang Y, Zhang FY, Liu KJ and Xiang B: Phenylephrine alleviates 131I damage in submandibular gland through promoting endogenous stem cell regeneration via lissencephaly-1 upregulation. Toxicol Appl Pharmacol 396: 114999, 2020.
44. He S, Li P, Zhong Q, Hou L, Yu Z, Huang Z, Chen X, Fang J and Chen X: Clinicopathologic and prognostic factors in adenoid cystic carcinoma of head and neck minor salivary glands: A clinical analysis of 130 cases. Am J Otolaryngol 38: 157-162, 2017.
45. Reiner O, Carrozzo R, Shen Y, Wehnert M, Faustinella F, Dobyns WB, Caskey CT and Ledbetter DH: Isolation of a Miller-Dieker lissencephaly gene containing G protein beta-subunit-like repeats. Nature 364: 717-721, 1993.
46. Kholmanskikh SS, Dobrin JS, Wynshaw-Boris A, Letourneau PC and Ross ME: Disregulated RhoGTPases and actin cytoskeleton contribute to the migration defect in Lis1-deficient neurons. J Neurosci 23: 8673-8681, 2003.
47. Miller LE, Au V, Mokhtari TE, Goss D, Faden DL and Varvares MA: A contemporary review of molecular therapeutic targets for adenoid cystic carcinoma. Cancers (Basel) 14: 992, 2022.
48. Biyanee A, Yusenko MV and Klempnauer KH: Src-family protein kinase inhibitors suppress MYB activity in a p300-dependent manner. Cells 11: 1162, 2022.
49. Ramsay NA and Glover BJ: MYB-bHLH-WD40 protein complex and the evolution of cellular diversity. Trends Plant Sci 10: 63-70, 2005.
50. Cao S, Lu X, Wang L, Qian X, Jin G and Ma H: The functional polymorphisms of LIS1 are associated with acute myeloid leukemia risk in a Han Chinese population. Leuk Res 54: 7-11, 2017.
51. Suzuki K and Takahashi K: Regulation of lamellipodia formation and cell invasion by CLIP-170 in invasive human breast cancer cells. Biochem Biophys Res Commun 368: 199-204, 2008.
52. Sipes NS, Feng Y, Guo F, Lee HO, Chou FS, Cheng J, Mulloy J and Zheng Y: Cdc42 regulates extracellular matrix remodeling in three dimensions. J Biol Chem 286: 36469-36477, 2011.
53. Yamaguchi H, Lorenz M, Kempiak S, Sarmiento C, Coniglio S, Symons M, Segall J, Eddy R, Miki H, Takenawa T and Condeelis J: Molecular mechanisms of invadopodium formation: The role of the N-WASP-Arp2/3 complex pathway and cofilin. J Cell Biol 168: 441-452, 2005.